Towards a universal exchange enhancement factor in density functional theory

C. M. Horowitz,[1] C. R. Proetto,[2,3] and J. M. Pitarke[4,5]

[1]*Instituto de Investigaciones Fisicoquímicas Teóricas y Aplicadas, UNLP, CCT La Plata-CONICET, Sucursal 4, Casilla de Correo 16, 1900 La Plata, Argentina*

[2]*Centro Atómico Bariloche and Instituto Balseiro, Universidad Nacional de Cuyo, 8400 S. C. de Bariloche, Río Negro, Argentina*

[3]*Instituto de Nanociencia y Nanotecnología, CONICET-CNEA, Sede Bariloche Av. Bustillo 9500 (8400) S. C. de Bariloche, Río Negro, Argentina*

[4]*CIC nanoGUNE BRTA, Tolosa Hiribidea 76, E-20018 Donostia, Basque Country, Spain*

[5]*Fisika Saila, Centro Física Materiales, CSIC-UPV/EHU, and DIPC, 644 Posta Kutxatila, E-48080 Bilbo, Basque Country, Spain*

(Received 16 September 2022; revised 25 March 2023; accepted 27 April 2023; published 11 May 2023)

A broadly used strategy to go beyond the well-known local-density approximation of density functional theory relies on the choice of a so-called exchange-correlation (xc) enhancement factor $F_{\rm xc}$, defined as the enhancement of a realistic xc energy density over its *local* exchange-only counterpart. To date, this density functional, $F_{\rm xc}$, has been constructed by following either semiempirical strategies or nonempirical schemes that impose the fulfillment of exact constraints. Here, we follow a totally different route, which is based on an attempt to construct a universal exchange enhancement factor F_x from the *exact* exchange energy density of a given family of electron density profiles and which we implement on the basis of jellium-slab exact-exchange self-consistent calculations. We find that such an enhancement factor can, indeed, be built which obeys, within our sample of electron-density profiles, most exact constraints and thus represents a *benchmark* towards the construction of a universal exchange enhancement factor suitable for all electron densities. We provide, in particular, an analytical parametrization of our *ab initio* calculations at the level of the generalized gradient approximation.

DOI: 10.1103/PhysRevB.107.195120

I. INTRODUCTION

Introduced in 1964, density functional theory (DFT) has become the method of choice for the calculation of the electronic structure of atoms, molecules, clusters, and solids [1–3], mainly due to a reasonable balance between accuracy and computational cost. DFT is also employed for the description of phonon excitations [4] and is now being widely used in the search for new materials with topological properties, a field with tremendous current activity [5]. Even the ubiquitous electron-phonon coupling [6] and the related superconducting state [7] are within the reach of first-principles calculations using suitable generalizations of DFT. Such generalizations include finite-temperature DFT [8] and time-dependent DFT [9], which allows for *ab initio* description of excited states.

In the framework of ground-state DFT, there is only one quantity that needs to be approximated, which is the exchange-correlation (xc) energy functional $E_{\rm xc}[n]$, known, for example, to represent the main ingredient of the glue that binds atoms together to form molecules and solids [10]. In their pioneering paper in 1965 [2], Kohn and Sham (KS) introduced the local-density approximation (LDA) by replacing, at each position $\mathbf{r}$, the *exact* xc energy density by the corresponding xc energy density of a uniform system with the *local* electron density $n(\mathbf{r})$. The next step beyond the LDA was to consider a second-order density-gradient expansion [11]. This approach, however, worsens the predictions of the LDA for real systems due to the fact that it does not inherit many of the exact constraints satisfied by the LDA. Some of these constraints were restored by a generalized gradient approximation (GGA) [12–15] and, later, by a more accurate meta-GGA (MGGA) [16–19]. While the LDA relies only on the knowledge of the local electron density $n(\mathbf{r})$, the GGA also relies on the knowledge of the local electron-density gradient $s(\mathbf{r}) = |\nabla n(\mathbf{r})|/[2(3\pi^2)^{1/3} n(\mathbf{r})^{4/3}]$, and the MGGA relies on both $s(\mathbf{r})$ and the parameter $\alpha(\mathbf{r})$ [20]. These approximations may be compactly expressed as follows:

$$E_{\rm xc}^{l}[n] = \int d\mathbf{r}\, n(\mathbf{r})\, \varepsilon_x^{\rm unif}(n(\mathbf{r}))\, F_{\rm xc}^{l}(n, s, \alpha, \dots), \qquad (1)$$

with $l =$ LDA, GGA, MGGA, etc. Here, $\varepsilon_x^{\rm unif}(n)$ represents the exchange energy per particle of a three-dimensional uniform system of electron density n: $\varepsilon_x^{\rm unif}(n) = -e^2(3/4\pi)(3\pi^2 n)^{1/3}$. The dimensionless density gradient $s(\mathbf{r})$ is zero for a uniform system, and as such it represents a measure of the system inhomogeneity. The MGGA parameter $\alpha(\mathbf{r})$ is easily found to be equal to 0 for a single-orbital two-electron density, equal to 1 for a uniform electron density, and very large in the case of weak bonds, so it can be taken to be a dimensionless deviation of an arbitrary many-electron system from single-orbital shape [21].

All GGA and MGGA xc energy functionals to date have been constructed by following two distinct routes: (i) semiempirical functionals, built to best reproduce existing data of real systems of interest (see, e.g., Refs. [13,16]), and (ii) nonempirical functionals, constructed by imposing the fulfillment of as many exact constraints as possible (see, e.g., Refs. [15,17–19]).

In this work, we follow a totally different approach, which is based on an attempt to construct a universal GGA or MGGA exchange enhancement factor F_x from the *exact* exchange energy density of a given family of electron-density profiles and which we implement on the basis of jellium-slab

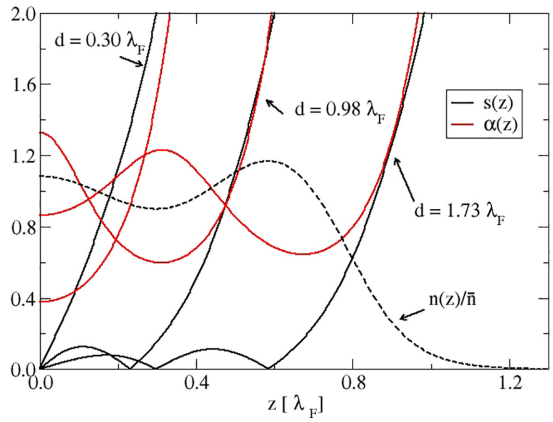

FIG. 1. $s(z)$ and $\alpha(z)$ (black and red solid lines) for $r_s = 6.0$ [27] and three slabs of increasing width: $d = 0.30\lambda_F, 0.98\lambda_F$, and $1.73\lambda_F$. The dashed line represents the normalized slab density $n(z)/\bar{n}$ for $d = 1.73\lambda_F$. $z = 0$ is always at the slab center.

exact-exchange self-consistent calculations [22–26] with two parameters: the jellium width d and the electron-density parameter r_s [27]. F_x represents the dominant contribution to the xc enhancement factor $F_{\rm xc} = F_x + F_c$ in the high-density ($r_s \to 0$) limit. We leave the *ab initio* building of F_c for future work.

Figure 1 shows plots of the density gradient $s(z)$ (black solid lines) and the MGGA parameter $\alpha(z)$ (red solid lines) for three slabs of increasing width. Since our slabs are symmetric with respect to the slab center, the density $n(z)$ always has zero slope at this point, which implies $s(z = 0) = 0$. In the case of the narrowest slab under consideration, which has one slab discrete level (SDL) occupied (SDL = 1), the ground-state density has no oscillations, thus leading to a density gradient $s(z)$ that monotonically increases from its zero value at the slab center as a consequence of the vanishing density in the denominator. On the other hand, $\alpha(z)$ has a finite value at the slab center and also increases monotonically in the vacuum region. For wider slabs with more than one occupied SDL, the electron density $n(z)$ exhibits the well-known Friedel oscillations inside the slab region, which lead to nodes of $s(z)$ at points of zero-slope density and also to an oscillatory behavior of $\alpha(z)$ around its bulk value $\bar{\alpha} = 1$. In the vacuum region, both $s(z)$ and $\alpha(z)$ increase exponentially for all jellium slabs. We note that the minimum value of α, which in the case of our narrowest slabs with SDL = 1 occurs at the center of the slab, decreases as the slab width decreases but reaches $\alpha = 0$ (which is the case for a single-orbital two-electron density) only when the electron gas collapses from three to two dimensions [28]. This regime is not addressed here, so our α parameter is never equal to zero, even when SDL = 1.

II. TOWARDS A UNIVERSAL FIRST-PRINCIPLES EXCHANGE ENHANCEMENT FACTOR

The exchange energy of an arbitrary many-electron system can be expressed as follows:

$$E_x[n] = \int d\mathbf{r}\, n(\mathbf{r})\, \varepsilon_x[n](\mathbf{r}), \tag{2}$$

where $\varepsilon_x[n](\mathbf{r})$ represents an exchange energy per particle, typically defined (conventional choice) as the interaction of a given electron at $\mathbf{r}$ with its own exchange hole. In the case of a jellium slab with translational invariance in a plane normal to the z axis, one writes [25]

$$\varepsilon_x^{\rm conv}[n](z) = \frac{-2\,e^2}{n(z)} \sum_{i,j}^{\rm occ} \gamma_{ij}(z) \int_{-\infty}^{\infty} dz' g_{ij}(|z - z'|)\, \gamma_{ji}(z'), \tag{3}$$

where $\gamma_{ij}(z) = \phi_i^*(z)\phi_j(z)$, with $\phi_i(z)$ and ε_i being the *occupied* eigenfunctions and eigenvalues of the effective one-dimensional (1D) exchange-only KS Hamiltonian [23] and $i = 1, 2, 3, \ldots$ being the SDL index. Also,

$$g_{ij}(u) = \frac{k_F^i k_F^j}{4\pi} \int_0^{\infty} \frac{d\rho}{\rho} \frac{J_1(\rho k_F^i) J_1(\rho k_F^j)}{\sqrt{\rho^2 + u^2}}, \tag{4}$$

with $J_1(x)$ being the cylindrical Bessel function of the first order and $k_F^i = \sqrt{2m_e(\mu - \varepsilon_i)}/\hbar$, with μ being the chemical potential, which is determined from the global neutrality condition. We obtain the single-particle orbitals $\phi_i(z)$ and energies ε_i by introducing the exchange-only version of the KS xc potential $v_{\rm xc}$ (Eq. (20) in Ref. [24]) into the effective 1D exchange-only KS Hamiltonian, which we then solve self-consistently. The ground-state electron density is simply $n(z) = \sum_i^{\rm occ} (k_F^i)^2 |\phi_i(z)|^2/2\pi$, where the factor $(k_F^i)^2/(2\pi)$ comes from the integration over the parallel (in the x-y plane) degrees of freedom.

A comparison of the exchange-only version of Eq. (1) with Eq. (2) leads us to define a *generalized* exchange enhancement factor as follows:

$$f_x[n](z) = \varepsilon_x[n](z)/\varepsilon_x^{\rm unif}(n(z)), \tag{5}$$

with the GGA and MGGA exchange enhancement factors $F_x^{\rm GGA} =: F_x(s)$ and $F_x^{\rm MGGA} =: F_x(s, \alpha)$ entering the exchange-only version of Eq. (1) being simply particular approximations of $f_x[n](z)$ [29].

The enhancement factors $F_x(s)$ and $F_x(s, \alpha)$ are expected to satisfy as many exact constraints as possible, with the aim of delivering the best possible approximation to $E_{\rm xc}[n]$. One of these exact constraints is the 3D Lieb-Oxford (LO) lower bound on the indirect part of the expectation value of the electron-electron interaction [30], which yields, in the case of an arbitrary spin-unpolarized electron density n, the inequality [31]

$$E_{\rm xc}[n] \geqslant B\, E_x^{\rm LDA}[n], \tag{6}$$

with $B = 1.804$. Recent work has found a tighter lower bond, $B = 1.3423$, when the wave function can be written as a single Slater determinant [32], while in the case of a spin-unpolarized two-electron ground state $B = 1.174$ has been found [21]. Similar lower bounds have been derived for the xc energy of a many-electron system in reduced dimensions [33].

The correlation energy is well known to never be positive, so the right-hand side of Eq. (6) also represents a lower bound on the exchange energy [31]:

$$E_x[n] \geqslant B\, E_x^{\rm LDA}[n], \tag{7}$$

which is fulfilled, at the level of the GGA or MGGA, if the respective enhancement factors $F_x(s)$ and $F_x(s,\alpha)$ satisfy

$$F_x(s), \quad F_x(s,\alpha) \leqslant B \tag{8}$$

for all s and α. Equation (8) is clearly a sufficient *local* condition for a GGA or MGGA to satisfy the *global* LO bound of Eq. (7). Perdew *et al.* [21] went further to point out that Eq. (8) is also a necessary condition if the exchange enhancement factor is to be universal, i.e., valid for all electron densities.

The *conventional* exchange energy per particle of Eq. (3) yields, however, $\varepsilon_x^{\rm conv}[n](z) \to -e^2/(2z)$ in the density tail of a jellium slab [25], so $f_x^{\rm conv}[n](z) = \varepsilon_x^{\rm conv}[n](z)/\varepsilon_x^{\rm unif}(n(z))$ diverges on the vacuum side of a jellium surface as $z \to \infty$ and cannot possibly be expressed as a *bounded* enhancement factor $F_x(s)$ or $F_x(s,\alpha)$ that fulfills Eq. (8) for all s and α, which occurs for other localized systems like helium and neon atoms [34] and the G2 set of molecules [35]. Nevertheless, this violation of the local form of the LO bound may be eliminated by simply introducing the following 1D coordinate transformation with $0 \leqslant \lambda < 1$ (see the Appendix):

$$\varepsilon_x^{\lambda}[n](z) = \frac{-2e^2}{n(z)} \sum_{i,j}^{occ.} \int_{-\infty}^{\infty} dz'\ \gamma_{ij}[(1+\lambda)z - \lambda z'] \times g_{ij}(|z-z'|)\gamma_{ji}[\lambda z + (1-\lambda)z'], \tag{9}$$

which also integrates to the total exchange energy of Eq. (2) [36]. This λ-dependent exchange energy per particle $\varepsilon_x^{\lambda}(z)$ is symmetric around $\lambda = 0.5$. When $\lambda = 0$, the conventional $\varepsilon_x^{\rm conv}(z)$ in Eq. (3) is recovered. The exchange enhancement factor $f_x^{\lambda}[n](z) = \varepsilon_x^{\lambda}[n](z)/\varepsilon_x^{\rm unif}(n(z))$ is found to diverge at $0 \leqslant \lambda < 0.25$ far outside the jellium surface into the vacuum, it tends at $\lambda = 0.25$ to a positive constant as $z \to \infty$, it remains bounded for all z at $0.25 \leqslant \lambda \leqslant 0.5$, and it exhibits the fastest decay at $\lambda = 0.5$ (see the Appendix). We find that, expressed as a function of the density gradient s, it decays as $s^{-1/2}$ in the large-s limit when the parameter $\lambda = 1/3$ (see the Appendix), thus fulfilling the high-density constraint describing the collapse of a system from three to two dimensions [21]. We also find that $\lambda = 1/3$ yields an exchange enhancement factor that is always below the local LO bound $B = 1.3423$, as shown in Fig. 2.

III. BUILDING OF THE GGA AND MGGA ENHANCEMENT FACTORS

First of all, we proceed with the construction of a GGA enhancement factor of the form $F_x(s)$ from a generalized $f_x^{\lambda}[n](z)$ with $\lambda = 1/3$. This generalized enhancement factor is, however, in general, not unique for each value of the density gradient s and all possible electron-density profiles, as it is a functional of the electron density $n(z)$. Our aim here is to build a GGA exchange enhancement factor $F_x(s)$ that is representative of all the values of $f_x^{\lambda=1/3}[n](z)$ that are found for a given s. With this purpose in mind, we proceed as follows: First, we calculate both $s(z)$ and $f_x^{\lambda=1/3}[n](z)$ for a large number of jellium slabs and within each slab for a large number of z coordinates. We have considered on the order of 1000 z coordinates and about 1500 jellium slabs with (i) r_s in the range of 2–20 and (ii) slab widths going from narrow slabs with $d \sim a_0$ to sufficiently wide slabs with $d \sim 100a_0$,

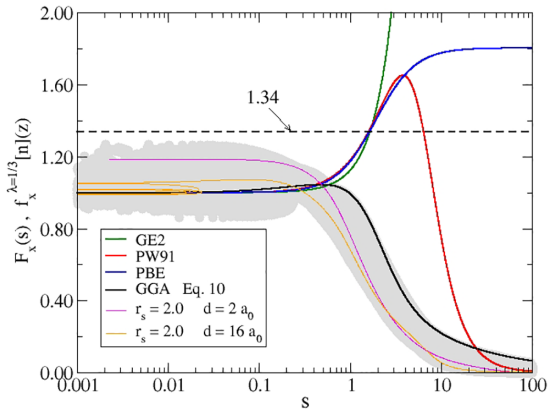

FIG. 2. GGA exchange enhancement factor $F_x(s)$ (black solid line), as obtained after the mappings $f_x^{\lambda}[n](z) \to f_x^{\lambda}(s) \to F_x(s)$, with $\lambda = 1/3$. The gray band here comprises *all* $f_x^{\lambda=1/3}(s)$ corresponding, at each s, to different ground-state electron-density profiles $n(z)$. It includes slabs with $r_s = 2, 6, 10, 20$ and illustrates the first mapping $f_x^{\lambda}[n](z) \to f_x^{\lambda}(s)$. The GGA $F_x(s)$ parametrization in Eq. (10), represented by a black solid line, corresponds to the second mapping $f_x^{\lambda}(s) \to F_x(s)$. Similar results are obtained for other values of the parameter λ in the range $0.25 < \lambda \leqslant 0.5$ (not shown here): while the lower bound of the gray band stays the same for all values of λ in this range, the upper bound increases as λ increases, with its minimum at $\lambda \approx 0.26$ and its maximum at $\lambda = 0.5$ slightly above the local LO bound $B = 1.3423$ (dashed line). The green solid curve represents the second-order gradient expansion (GE2) $F_x^{\rm GE2}(s \to 0) = 1 + \mu_{\rm GE2}\, s^2$, with $\mu_{\rm GE2} = 10/81$ [37]. The red and blue solid curves represent well-known GGAs: $F_x^{\rm PW91}(s)$ [38] (red line) and $F_x^{\rm PBE}(s)$ [15] (blue line). The remaining curves (pink and yellow) are explained in the text.

with a_0 being the Bohr radius. We find that, depending on the electron-density profile $n(z)$, there are, in general, a number of values of $f_x^{\lambda=1/3}[n](z)$ corresponding to the very same density gradient s, as expected. They all lie, however, within a very well defined band (gray area in Fig. 2), which always stays below the LO bound $B = 1.3423$; we symbolize this first step as the $f_x^{\lambda}[n](z) \to f_x^{\lambda}(s)$ mapping. This allows us to define, as a second step and within this band, a parameterized GGA enhancement factor $F_x(s)$ (black solid line in Fig. 2), which we have constructed in such a way that the uniform-density limit $F_x(s \to 0) \to 1 + \mu_{\rm GE2}\, s^2$ and the large-s limit $F_x(s \gg 1) \to s^{-1/2}$ are both guaranteed. We symbolize this second step as the $f_x^{\lambda}(s) \to F_x(s)$ mapping. Our explicit GGA $F_x(s)$ parametrization is as follows:

$$F_x(s) = \frac{1 + 10s^2/81}{1 + 0.19s^{2.5} - 0.01\ln(1+400s^2)}. \tag{10}$$

In Fig. 2, we plot this parametrization together with the second-order gradient expansion (GE2) and two well-known GGAs: Perdew-Wang 91 (PW91) and Perdew-Burke-Ernzerhof (PBE). These approximations (GE2, PW91, and PBE) all violate the local LO bound, and none of them behaves as $s^{-1/2}$ at large s. We also include two examples of the first mapping $f_x^{\lambda}[n](z) \to f_x^{\lambda}(s)$ by plotting $f_x^{\lambda}(s)$ for two particular slabs: (i) a narrow slab with one SDL occupied, which exhibits a one-to-one correspondence between s and z (see Fig. 1) and therefore a single-valued function $f_x^{\lambda}(s)$

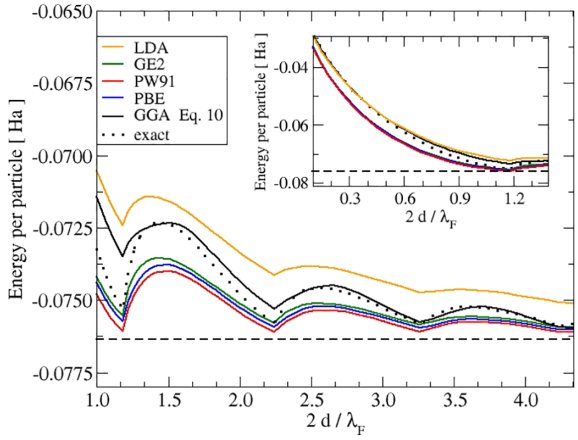

FIG. 3. Exact E_x/N versus the slab width $2d/\lambda_F$ (black dotted line) for $r_s = 6$, together with the result we obtain with the GGA parametrization in Eq. (10) (black solid line) and also the LDA (yellow solid line), GE2 (green solid line), and the standard GGAs PW91 (red solid line) and PBE (blue solid line). The horizontal dashed line denotes the bulk $d \to \infty$ result $\bar{E}_x/N = -(3/4\pi)(9\pi/4)^{1/3} r_s^{-1}$.

(pink solid line), and (ii) a wider slab with SDL = 5 exhibiting a multivalued $f_x^\lambda(s)$ function at low values of the density gradient s (yellow solid line). We have recalculated the mapping $f_x^\lambda[n](z) \to f_x^\lambda(s)$ for these two particular slabs by using a self-consistent ground-state electron density that includes LDA correlation [39], and we have found results that are indistinguishable to the naked eye, as expected.

Figure 2 clearly shows that for a narrow slab (pink solid line) the uniform-density limit is never reached for small values of s. As our GGA parametrization (black solid line) is constructed to fulfill the uniform-density limit, it cannot possibly reproduce the exchange enhancement factor $f_x^\lambda(s)$ for narrow slabs. For the calculation of integrated quantities, like the exchange energy per particle (see Fig. 3), this shortcoming can be compensated by a particular choice of the second and third terms in the denominator of Eq. (10), which results in an increase in our parameterized exchange enhancement factor, still within the gray area, for $s \geqslant 0.6$.

With the aim of testing the accuracy of our GGA parametrization, we have inserted Eq. (10) into Eq. (1) in order to obtain a GGA exchange energy per particle $E_x^{\rm GGA}/N$, as shown in Fig. 3. For comparison, also included in Fig. 3 the exact optimized effective potential (OEP) exchange energy per particle (black dotted line) and the results obtained by using the three parametrizations in Fig. 2, GE2, PW91, and PBE, as well as the LDA. The exchange energy per particle oscillates, as expected, and approaches the corresponding bulk value from above, with local minima each time a new subband for the z motion becomes occupied, which happens at specific values of the slab width d. This oscillatory behavior reflects the competition between intrasubband exchange (dominant at high occupancy of the last occupied subband) and intersubband exchange (dominant at low occupancy of the last occupied subband). As is usually the case, the LDA overestimates the exchange energy, which is, to some extent, overcorrected by the GE2 and the GGAs under study (PW91 and PBE), thus leading to an underestimation of E_x/N. Our *ab initio* constructed GGA corrects the LDA substantially and get, for most slabs, very close to the exact E_x/N; it is only for those slab widths for which a new subband starts to be occupied that our GGA overestimates the exact result. We conclude that our *ab initio* approach allows for the construction of a parameterized GGA, leading, overall, to accurate total exchange energies for the electron densities under study.

To construct a MGGA enhancement factor $F_x(s,\alpha)$, we proceed in a similar way, but with a different protocol for the construction of the second mapping. We first calculate $s(z)$, $\alpha(z)$, and $f_x^{\lambda=1/3}[n](z)$ for the same jellium slabs and z coordinates as in the case of the GGA. We find that, depending on the electron-density profile $n(z)$, there are, in general, still various exchange enhancement factors corresponding to the same (s,α), again as expected, but now within much narrower bands, as shown in the top panels of Figs. 4 and 5, which always stay below the LO bound $B = 1.3423$. This is the $f_x^\lambda[n](z) \to f_x^\lambda(s,\alpha)$ mapping. Then we perform, for each value of the parameters s and α, a *simple* average over the results that we obtain for all z coordinates (and jellium slabs) leading to those particular values of s and α. This average yields the exchange enhancement factor $F_x(s,\alpha)$ that we plot with solid lines in the bottom panels of Figs. 4 and 5 for various values of α as a function of s (Fig. 4) and as a function of α for various values of s (Fig. 5). This is the $f_x^\lambda(s,\alpha) \to F_x(s,\alpha)$ mapping.

We note that due to the intrinsic features of our electron-density profiles, (i) the emerging α parameter displays a natural clustering around $\alpha \sim 1$ for small s (uniform limit), (ii) larger values of α are found only when s is large [40], (iii) intermediate values of s [typically around the jellium-vacuum interface with (s,α) represented by the crosses in the bottom panel of Fig. 4] occur only when $\alpha \lesssim 1$, and (iv) only electron-density profiles corresponding to thin jellium slabs in the SDL = 1 regime allow for small values of the parameter α (see also Fig. 1). Furthermore, it is precisely for these small values of α that one value of the exchange enhancement factor $f_x^{\lambda=1/3}[n](z)$ is found for each (s,α), thus providing, for $\alpha < 1$, a unique definition of the MGGA enhancement factor $F_x(s,\alpha)$.

Figure 4 shows very clearly that for the smallest value of α under study ($\alpha = 0.3$), $F_x(s,\alpha)$ stays below the very tight local bound $B = 1.174$ for all s, which was shown by Perdew *et al.* [21] to hold at $\alpha = 0$. Perdew *et al.* [21] went further to conjecture that the very tight bound $B = 1.174$ should still hold for all $\alpha > 0$ since the enhancement factor was expected to decrease as α increases [21]. This is, however, not what we find here. In the case of large slabs (semi-infinite jellium), we do find an exchange enhancement factor $F_x(s,\alpha)$ that decreases monotonically with α, but this monotonic decrease does not occur in the case of thin jellium slabs due to finite-size effects. Indeed, Figs. 4 and 5 show that the enhancement factor $F_x(s,\alpha)$ for small s first increases for values of α going from $\alpha \simeq 0.3$ to $\alpha \simeq 0.5$, still below the local LO bound $B = 1.3423$ but above $B = 1.174$, and then decreases for larger values of α. Similar results to those exhibited in Figs. 4 and 5 for $r_s = 6$ are obtained for the other r_s values under study: $r_s = 2, 10, 20$.

Figures 4 and 5 also show that at low values of the density gradient s [typically corresponding to z coordinates inside the

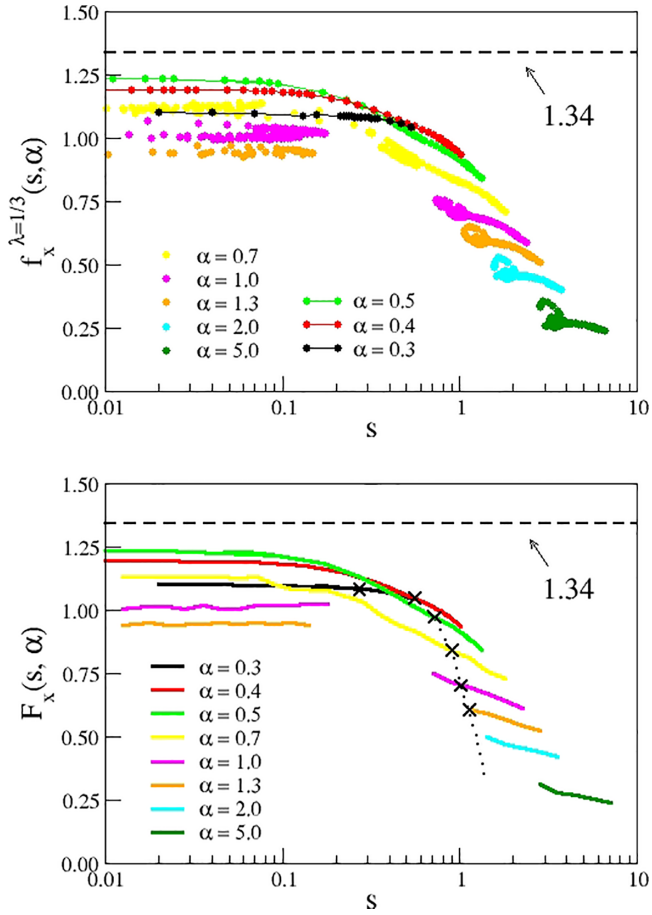

FIG. 4. The bottom panels shows the MGGA exchange enhancement factor $F_x(s,\alpha)$ (solid lines), as obtained after the mappings $f_x^\lambda[n](z) \to f_x^\lambda(s,\alpha) \to F_x(s,\alpha)$, with $\lambda = 1/3$, $r_s = 6$, and various values of α as a function of s. The top panel, which illustrates the first mapping $f_x^\lambda[n](z) \to f_x^\lambda(s,\alpha)$, comprises all $f_x^{\lambda=1/3}(s,\alpha)$ corresponding, at each (s,α), to different ground-state electron-density profiles $n(z)$. Our *average* MGGA exchange enhancement factor $F_x(s,\alpha)$, represented by solid lines in the bottom panel, corresponds to the second mapping $f_x^\lambda(s,\alpha) \to F_x(s,\alpha)$. The crosses joined by the dotted line in the bottom panel represent the (s,α) parameters corresponding to a z coordinate at the jellium-vacuum interface. The dashed line represents the local LO bound $B = 1.3423$.

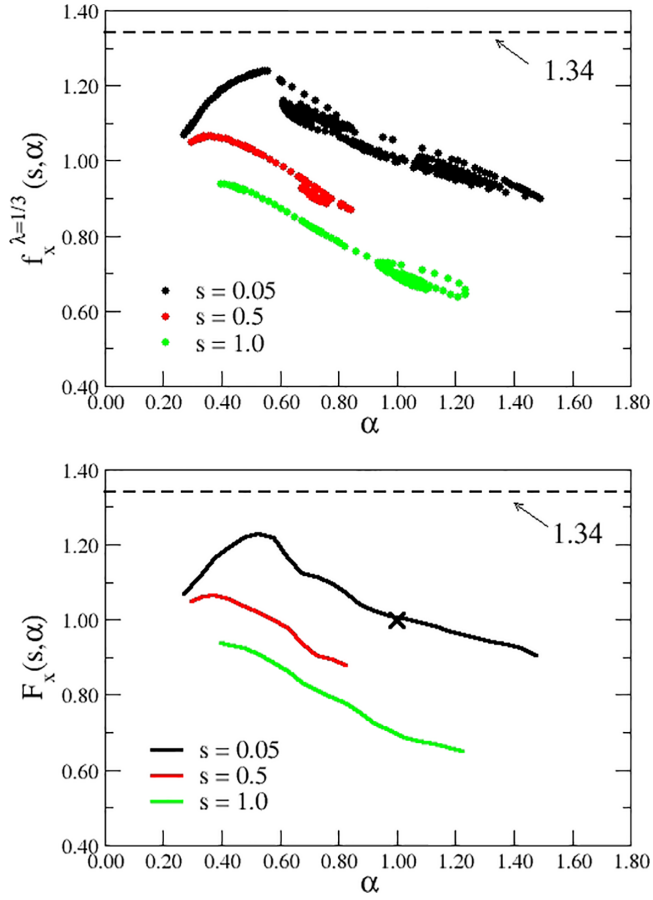

FIG. 5. Same as Fig. 4, but now as a function of α for various values of s. The cross in the bottom panel denotes the uniform-gas MGGA exchange enhancement factor $F_x = 1$ that is expected to occur at $s = 0$ and $\alpha = 1$.

slab, where the electron density $n(z)$ becomes increasingly uniform as the slab center is approached], the exchange enhancement factor is a very well defined function of s an α, while at larger values of s (typically corresponding to z coordinates on the vacuum side of the surface where the electron density decreases considerably) various values of $f_x^{\lambda=1/3}$ correspond to the same parameters s and α, although still within a narrow band. This is an expected result, as it is precisely in this region where the use of the MGGA is less justified, but the fact that all different values of the exchange factor for given values of s and α stay within narrow bands indicates that the MGGA scheme is still expected to represent a good approximation for the electron-density profiles under study.

The lack of data in Figs. 4 and 5 for $\alpha \to 0$ precludes us from providing a MGGA parametrization of the exchange enhancement factor $F_x(s,\alpha)$. The reason for this is that small values of α can be obtained only when the electron gas collapses from three to two dimensions, i.e., by keeping the electron density constant in two dimensions as the jellium slab gets thinner, which is beyond our scope here. Work in this direction is now in progress.

IV. CONCLUSIONS

In summary, we have reported an *ab initio* attempt to construct universal GGA and MGGA exchange enhancement factors based on a family of jellium-slab exact-exchange self-consistent calculations. We found that both $F_x(s)$ and $F_x(s,\alpha)$ lie within very well defined bands that stay, for all s and α, below the local form of the Lieb-Oxford bound $B = 1.3423$ reported very recently for a situation where the wave function can be written as a single Slater determinant [32]. In the case of the GGA, our *first-principles* calculations allow us to devise a parametrization of $F_x(s)$ that yields very accurate exchange energies per particle. In the case of the MGGA exchange enhancement factor, we find that (i) for small values of α ($\alpha = 0.3$) $F_x(s,\alpha)$ stays, for all s, below the very tight bound $B = 1.174$, which was found in Ref. [21] to hold in the case of a spin-unpolarized two-electron ground state with $\alpha = 0$, (ii) for small s and values of α such that $0.3 \lesssim \alpha \lesssim 0.5$ the enhancement factor $F_x(s,\alpha)$ increases, due to the presence

of finite-size effects, above the very-tight bound $B = 1.174$ but is still below the LO bound $B = 1.3423$, and (iii) for larger values of α the exchange enhancement factor decreases monotonically with α. For $\alpha = 1$ and low values of the density gradient s, $F_x(s, \alpha) \to 1$, showing that in this regime the exact exchange energy per particle approaches the exchange energy per particle of a uniform electron gas at local density, as expected.

We believe that our *ab initio* construction of exchange enhancement factors $F_x(s)$ and $F_x(s, \alpha)$ represents a benchmark towards the construction of a universal exchange enhancement factor suitable for all electron densities. A similar scheme could be used, in principle, for the *ab initio* construction of xc enhancement factors $F_{\rm xc}(s)$ and $F_{\rm xc}(s, \alpha)$. A suitable starting point could be to follow the procedure described in Ref. [41] to investigate the electronic subband structure of semiconductor quantum wells, where carriers are free to move within a plane while being confined in the remaining direction.

ACKNOWLEDGMENTS

We thank UnCaFiQT (SNCAD) for computational resources and J. P. Perdew for insightful discussions. C.M.H. wishes to acknowledge the financial support received from CONICET of Argentina through Grant No. PIP 2014-47029. C.R.P. wishes to acknowledge the financial support received from CONICET and ANPCyT of Argentina through Grants No. PIP 2014-47029 and No. PICT 2016-1087.

APPENDIX

In this Appendix, we present the derivation of the one-dimensional (1D) coordinate transformation of Eq. (9), as well as proof of the invariance of the Kohn-Sham (KS) exact-exchange potential $v_x[n](z)$ under this transformation and the derivation of the large-s limit, $F_x(s \gg 1) \sim s^{-1/2}$.

1. Derivation of Equation (9)

In the case of a jellium slab with translational invariance in a plane normal to the z axis, the exchange energy functional $E_x[n]$ can be written as follows [26]:

$$E_x[n] = \pi e^2 A \int_{-\infty}^{\infty} dz\, n(z) \int_0^{\infty} \rho d\rho \int du\, \frac{h_x(z; \rho, z+u)}{(\rho^2+u^2)^{1/2}}, \tag{A1}$$

with

$$h_x(z; \rho, z+u) = \frac{-1}{2n(z)} \left| \sum_i^{\rm occ} \frac{k_F^i J_1\left(\rho k_F^i\right)}{\pi \rho} \phi_i(z) \phi_i^*(z+u) \right|^2 \tag{A2}$$

being the exchange hole density at coordinate $(\rho, z+u)$ (observational point) due to the presence of an electron at coordinate $(0, z)$.

We proceed now by performing the appropriate 1D transformation $(z, z+u) \to (z_1, z_2)$, where $z = az_1 + bz_2$ and $z + u = cz_1 + dz_2$, with a, b, c, and d being constants to be fixed. As in Ref. [21], but now transforming only in one dimension, we impose that $u = z_2 - z_1$ and $J(a, b, c, d) = ad - bc = 1$, with J being the Jacobian of the coordinate transformation. We obtain the solution $a = 2 - d$, $b = d - 1$, and $c = 1 - d$. Also, $z = (2-d)z_1 + (d-1)z_2 = z_1 + u(d-1)$, and $z + u = (1-d)z_1 + z_2 d = z_1 + ud$. Under this 1D transformation, Eq. (A1) yields

$$\begin{aligned} E_x[n] &= -\frac{e^2 A}{2\pi} \int dz_1 \int du \int_0^{\infty} \frac{d\rho}{\rho(\rho^2+u^2)^{1/2}} \\ &\quad \times \left| \sum_i^{\rm occ} k_F^i J_1\left(\rho k_F^i\right) \phi_i[z_1 + u(d-1)] \phi_i^*(z_1 + ud) \right|^2 \\ &=: A \int_{-\infty}^{\infty} dz_1\, n(z)\, e_x^d[n](z_1), \end{aligned} \tag{A3}$$

with $\varepsilon_x^d[n](z) = e_x^d[n](z)/n(z)$ being the "d-transformed" exchange energy per particle of Eq. (9). Under a change in integration variables, one finds that $E_x[n]$ does not depend on the parameter d, as expected. In the main text, we have taken $d = \lambda$.

2. Invariance of $v_x[n](z)$

Here, we show that the KS exact-exchange potential $v_x[n](z)$ remains invariant under the 1D coordinate transformation described in the previous section, as expected. For the sake of simplicity, we assume that only one slab discrete level is occupied, i.e., SDL = 1. In this case, Eq. (A3) can be written as follows:

$$\begin{aligned} E_x[n] = -\frac{8\pi^2 e^2 A}{(k_F^1)^2} \int dz \int dz'\, n(z + \lambda z')\, g_{11}(|z'|) \\ \times n[z + (\lambda - 1)z']. \end{aligned} \tag{A4}$$

As the exchange energy of Eq. (A4) is an explicit functional of the electron density $n(z)$, the derivation of the corresponding Kohn-Sham exchange potential is straightforward:

$$\begin{aligned} v_x^{\lambda}[n](z) &= \frac{1}{A} \frac{\delta E_x}{\delta n(z)} = -\frac{8\pi^2 e^2}{\left(k_F^1\right)^2} \int dz_1 \int dz_2\, g_{11}(|z_2|) \\ &\quad \times \{n(z_1 + \lambda z_2)\, \delta[z - z_1 - (\lambda - 1)z_2] \\ &\quad + n[z_1 + (\lambda - 1)z_2]\, \delta(z - z - \lambda z_2)\} \\ &= -\frac{8\pi^2 e^2}{\left(k_F^1\right)^2} \int dz_2\, g_{11}(|z_2|)[n(z + z_2) + n(z - z_2)] \\ &= -\frac{16\pi^2 e^2}{\left(k_F^1\right)^2} \int dz_2\, g_{11}(|z_2|) n(z + z_2) \\ &= -\frac{16\pi^2 e^2}{\left(k_F^1\right)^2} \int dz' g_{11}(|z - z'|)\, n(z'). \end{aligned} \tag{A5}$$

In passing from Eq. (A4) to the first line in Eq. (A5), we have used the functional derivative rule $\delta f(x)/\delta f(x') = \delta(x - x')$. Clearly, $v_x^{\lambda}[n](z)$ does not depend on the parameter λ. In addition, taking into account that [26]

$$g_{11}(|z|) = \frac{\left(k_F^1\right)^2}{8\pi |z|} \left[1 - \frac{I_1\left(2k_F^1 |z|\right)}{k_F^1 |z|} + \frac{L_1\left(2k_F^1 |z|\right)}{k_F^1 |z|} \right], \tag{A6}$$

the well-known expression for the SDL = 1 KS exchange potential is recovered [24]. $I_1(x)$ and $L_1(x)$ entering Eq. (A6)

represent the modified Bessel and Struve functions, respectively.

3. Asymptotic analysis of the exchange enhancement factor

We start by introducing a change in the integration variable z' in Eq. (9) by setting $t = \lambda z + (\lambda - 1)z'$. Equation (9) may then be rewritten as follows:

$$\varepsilon_x^\lambda[n](z) = \frac{-2e^2}{n(z)} \sum_{i,j}^{occ.} \int_{-\infty}^{\infty} \frac{dt}{1-\lambda}\, \gamma_{ij} \times \left(\frac{z-\lambda t}{1-\lambda}\right) g_{ij}\left(\left|\frac{z-t}{1-\lambda}\right|\right) \gamma_{ji}(t). \quad \text{(A7)}$$

In the asymptotic limit $z \to \infty$ (far deep into the vacuum region), the KS orbitals whose arguments are $(z - \lambda t)/(1 - \lambda)$ collapse to the case $i = j = M$, with M being the last occupied SDL, which is the one with the slowest decay length. This leads to the following simplification of Eq. (A7):

$$\varepsilon_x^\lambda[n](z \to \infty) \to \frac{-2e^2}{n(z \to \infty)} \int_{-\infty}^{\infty} \frac{dt}{1-\lambda}\, \gamma_{MM} \times \left(\frac{z-\lambda t}{1-\lambda}\right) g_{MM}\left(\left|\frac{z-t}{1-\lambda}\right|\right) \gamma_{MM}(t). \quad \text{(A8)}$$

Assuming now an exponential decay for the last occupied KS orbital, $n(z \to \infty) \sim |\xi_M(z \to \infty)|^2 = \gamma_{MM}(z \to \infty) \sim e^{-2z\beta_M}$, Eq. (A8) may be estimated, to exponential accuracy, as follows:

$$\varepsilon_x^\lambda[n](z \to \infty) \sim e^{2z\beta_M} e^{-2z\beta_M/(1-\lambda)} = e^{-2z\beta_M\lambda/(1-\lambda)}, \quad \text{(A9)}$$

with the λ-dependent exponential factor being the estimated contribution of the factor $\gamma_{MM}[(z - \lambda t)/(1 - \lambda)]$, after taking it outside the integral by neglecting the contribution proportional to λt inside its argument.

Returning now to Eq. (5), we obtain the following estimate:

$$f_x^\lambda[n](z \to \infty) = \frac{\varepsilon_x^\lambda[n](z \to \infty)}{\varepsilon_x^{\text{unif}}(n(z \to \infty))} \sim \frac{e^{-2z\beta_M\lambda/(1-\lambda)}}{e^{-2z\beta_M/3}} = e^{-2z\beta_M\{(4\lambda-1)/[3(1-\lambda)]\}}. \quad \text{(A10)}$$

For $f_x^\lambda[n](z \to \infty)$ to remain finite, the quantity $4\lambda - 1$ should be greater than zero, which implies $\lambda > 0.25$. In particular, for $\lambda = 1/3$ one obtains:

$$f_x^{\lambda=1/3}[n](z \to \infty) \sim e^{-z\beta_M/3}. \quad \text{(A11)}$$

From the asymptotic analysis of $s(z)$, at large z we find $z \to (3/2\beta_M)\ln[s(z)]$. Introducing this into Eq. (A11), we find the large-s limit $f_x^{\lambda=1/3}[n](z \to \infty) \sim F_x(s \to \infty) \sim s^{-1/2}$.

[1] P. Hohenberg and W. Kohn, Inhomogeneous electron gas, Phys. Rev. **136**, B864 (1964).

[2] W. Kohn and L. J. Sham, Self-consistent equations including exchange and correlation effects, Phys. Rev. **140**, A1133 (1965).

[3] E. Engel and R. M. Dreizler, *Density Functional Theory: An Advanced Course* (Springer, Berlin, 2011).

[4] S. Baroni, S. de Gironcoli, A. dal Corso, and P. Giannozzi, Phonons and related crystal properties from density-functional perturbation theory, Rev. Mod. Phys. **73**, 515 (2001).

[5] A. Bansil, H. Lin, and T. Das, Colloquium: Topological band theory, Rev. Mod. Phys. **88**, 021004 (2016).

[6] F. Giustino, Electron-phonon interactions from first principles, Rev. Mod. Phys. **89**, 015003 (2017).

[7] A. Sanna, Introduction to superconducting density functional theory, https://www.cond-mat.de/events/correl17/manuscripts/sanna.pdf.

[8] N. D. Mermin, Thermal properties of the inhomogeneous electron gas, Phys. Rev. **137**, A1441 (1965).

[9] *Fundamentals of Time-Dependent Density Functional Theory*, edited by M. A. L. Marques, N. T. Maitra, F. M. S. Nogueira, E. K. U. Gross, and A. Rubio (Springer, Heidelberg, 2012).

[10] S. Kurth and J. P. Perdew, Role of the exchange-correlation energy: Nature's glue, Int. J. Quantum Chem. **77**, 814 (2000).

[11] M. Rasolt and D. J. W. Geldart, Gradient Corrections in the Exchange and Correlation Energy of an Inhomogeneous Electron Gas, Phys. Rev. Lett. **35**, 1234 (1975).

[12] D. C. Langreth and M. J. Mehl, Beyond the local-density approximation in calculations of ground-state electronic properties, Phys. Rev. B **28**, 1809 (1983).

[13] A. D. Becke, Density-functional exchange-energy approximation with correct asymptotic behavior, Phys. Rev. A **38**, 3098 (1988).

[14] J. P. Perdew, J. A. Chevary, S. H. Vosko, K. A. Jackson, M. R. Pederson, D. J. Singh, and C. Fiolhais, Atoms, molecules, solids, and surfaces: Applications of the generalized gradient approximation for exchange and correlation, Phys. Rev. B **46**, 6671 (1992); Erratum: Atoms, molecules, solids, and surfaces: Applications of the generalized gradient approximation for exchange and correlation, **48**, 4978(E) (1993).

[15] J. P. Perdew, K. Burke, and M. Ernzerhof, Generalized Gradient Approximation Made Simple, Phys. Rev. Lett. **77**, 3865 (1996).

[16] A. Becke, A new inhomogeneity parameter in density-functional theory, J. Chem. Phys. **109**, 2092 (1998).

[17] J. P. Perdew, S. Kurth, A. Zupan, and P. Blaha, Accurate Density Functional with Correct Formal Properties: A Step Beyond the Generalized Gradient Approximation, Phys. Rev. Lett. **82**, 2544 (1999).

[18] J. Sun, A. Ruzsinsky, and J. P. Perdew, Strongly Constrained and Appropriately Normed Semilocal Density Functional, Phys. Rev. Lett. **115**, 036402 (2015).

[19] T. Aschebrock and S. Kümmel, Ultranonlocality and accurate band gaps from a meta-generalized gradient approximation, Phys. Rev. Res. **1**, 033082 (2019).

[20] $\alpha(\mathbf{r}) = [t(\mathbf{r}) - t^{\mathrm{W}}(\mathbf{r})]/t^{\mathrm{unif}}(\mathbf{r}) \geqslant 0$, where t is the kinetic-energy density, $t^{\mathrm{W}} = |\nabla n|^2/8n$ is its von Weizsäcker counterpart, and $t^{\mathrm{unif}} = (3/10)(3\pi^2)^{2/3}n^{5/3}$ is the kinetic-energy density of a three-dimensional uniform electron gas. Since t^{W} is a lower bound of t [42], $\alpha \geqslant 0$.

[21] J. P. Perdew, A. Ruzsinszky, J. Sun, and K. Burke, Gedanken densities and exact constraints in density functional theory, J. Chem. Phys. **140**, 18A533 (2014).

[22] C. Horowitz, C. R. Proetto, and J. M. Pitarke, Semilocal approximations to the Kohn-Sham exchange potential as applied to a metal surface, Phys. Rev. B **105**, 085149 (2022).

[23] C. M. Horowitz, S. Rigamonti, and C. R. Proetto, Kohn-Sham Exchange Potential for a Metallic Surface, Phys. Rev. Lett. **97**, 026802 (2006).

[24] C. M. Horowitz, C. R. Proetto, and J. M. Pitarke, Exact-exchange Kohn-Sham potential, surface energy, and work function of jellium slabs, Phys. Rev. B **78**, 085126 (2008).

[25] C. M. Horowitz, L. A. Constantin, C. R. Proetto, and J. M. Pitarke, Position-dependent exact-exchange energy for slabs and semi-infinite jellium, Phys. Rev. B **80**, 235101 (2009).

[26] C. Horowitz, C. R. Proetto, and J. M. Pitarke, Asymptotics of the metal-surface Kohn-Sham exact exchange potential revisited, Phys. Rev. B **104**, 155108 (2021).

[27] The dimensionless electron-density parameter r_s is given by $r_s = (3/4\pi\bar{n})^{1/3}$, in units of the Bohr radius a_0, with $\bar{n}$ being the uniform density of the jellium background. Also, $\lambda_F/a_0 = 2\pi/(a_0 k_F) = 2\pi/(3\pi^2\bar{n})^{1/3} = (32\pi^2/9)^{1/3}\, r_s$.

[28] A. D. Kaplan, K. Wagle, and J. P. Perdew, Collapse of the electron gas from three to two dimensions in Kohn-Sham density functional theory, Phys. Rev. B **98**, 085147 (2018).

[29] The exchange enhancement factors $F_x(s)$ and $F_x(s,\alpha)$ are known not to depend on the local electron density, thus satisfying the constraint $E_x[n_\gamma] = \gamma E_x[n]$ under uniform scaling, i.e., with $n_\gamma(\mathbf{r}) = \gamma^3 n(\gamma\mathbf{r})$ [43].

[30] E. H. Lieb and S. Oxford, Improved lower bound on the indirect Coulomb energy, Int. J. Quantum Chem. **19**, 427 (1981).

[31] J. P. Perdew, Unified theory of exchange and correlation beyond the local density approximation, in *Electronic Structure of Solids'91*, edited by P. Ziesche and H. Eshrig (Akademie Verlag, Berlin, 1991), p. 11.

[32] M. Lewin, E. H. Lieb, and R. Seiringer, Improved Lieb-Oxford bound on the indirect and exchange energies, Lett. Math. Phys. **112**, 92 (2022).

[33] E. Räsänen, S. Pittalis, K. Capelle, and C. R. Proetto, Lower Bounds on the Exchange-Correlation Energy in Reduced Dimensions, Phys. Rev. Lett. **102**, 206406 (2009).

[34] D. J. Lacks and R. G. Gordon, Pair interactions of rare-gas atoms as a test of exchange-energy-density functionals in regions of large density gradients, Phys. Rev. A **47**, 4681 (1993).

[35] J. G. Vilhena, E. Räsänen, L. Lehtovaara, and M. L. Marques, Violation of a local form of the Lieb-Oxford bound, Phys. Rev. A **85**, 052514 (2012).

[36] J. Tao, M. Sprinborg, and J. P. Perdew, Properties of the exchange hole under an appropriate coordinate transformation, J. Chem. Phys. **119**, 6457 (2003).

[37] P. R. Antoniewicz and L. Kleimann, Kohn-Sham exchange potential exact to first order in $\rho(\mathbf{K})/\rho_0$, Phys. Rev. B **31**, 6779 (1985).

[38] K. Burke, J. P. Perdew, and Y. Wang, Derivation of a generalized gradient approximation: The PW91 density functional, in *Electronic Density Functional Theory*, edited by J. F. Dobson, G. Vignale, and M. P. Das (Springer, Berlin, 1998).

[39] N. D. Lang and W. Kohn, Theory of metal surfaces: Charge density and surface energy, Phys. Rev. B **1**, 4555 (1970).

[40] This may be understood by rewriting α as $\alpha = t/t^{\mathrm{unif}} - 5s^2/3 \geqslant 0$ because at $s \gg 1$ (the vacuum region) α (which is never negative) should scale at least as As^2 with $A \geqslant 5/3$.

[41] S. Rigamonti and C. R. Proetto, Signature of Discontinuity in the Exchange-Correlation Energy Functional Derived from Subband Electronic Structure of Semiconductor Quantum Wells, Phys. Rev. Lett. **98**, 066806 (2007).

[42] S. Kurth, J. P. Perdew, and P. Blaha, Molecular and solid-state tests of density functional approximations: LSD, GGAs, and meta-GGAs, Int. J. Quantum Chem. **75**, 889 (1999).

[43] M. Levy and J. P. Perdew, Hellmann-Feynman, virial, and scaling requisites for the exact universal density functionals. Shape of the correlation potential and diamagnetic susceptibility for atoms, Phys. Rev. A **32**, 2010 (1985).